eScience 3 (2023) 100139

Contents lists available at ScienceDirect

eScience

journal homepage: www.keaipublishing.com/en/journals/escience

Perspective

Heterostructure engineering in electrode materials for sodium-ion batteries: Recent progress and perspectives

Eric Gabriel [a,b,1], Chunrong Ma [c,d,1], Kincaid Graff [a], Angel Conrado [a], Dewen Hou [a,e], Hui Xiong [a,f,*]

[a] Micron School of Materials Science and Engineering, Boise State University, Boise, ID, 83725, USA
[b] X-ray Sciences Division, Argonne National Laboratory, Lemont, IL, 60439, USA
[c] College of Textiles & Clothing, Qingdao University, Qingdao, 266071, China
[d] Key Laboratory of Bio-Fibers and Eco-Textiles, Qingdao University, Qingdao, 266071, China
[e] Center for Nanoscale Materials, Argonne National Laboratory, Lemont, IL, 60439, USA
[f] Center for Advanced Energy Studies, Idaho Falls, ID, 83401, USA

HIGHLIGHTS

- Heterostructure engineering offers new avenues to tune electrode properties.
- The phase interface alters local electrode properties, with long-range effects.
- Efficient methods for heterostructure synthesis are reviewed.
- The origin of the heterostructure's influence on electrode properties is discussed.
- Future challenges and opportunities for heterostructure engineering are considered.

GRAPHICAL ABSTRACT

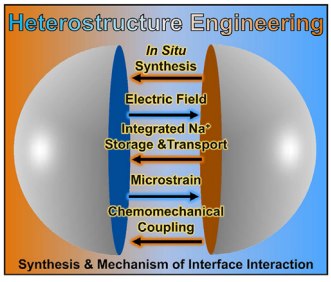

ARTICLE INFO

Keywords:
Heterostructure
Sodium-ion batteries
Electrode materials
Heterogeneous materials
Interface engineering
Intergrowth

ABSTRACT

Sodium-ion batteries (SIBs) have stepped into the spotlight as a promising alternative to lithium-ion batteries for large-scale energy storage systems. However, SIB electrode materials, in general, have inferior performance than their lithium counterparts because Na^+ is larger and heavier than Li^+. Heterostructure engineering is a promising strategy to overcome this intrinsic limitation and achieve practical SIBs. We provide a brief review of recent progress in heterostructure engineering of electrode materials and research on how the phase interface influences Na^+ storage and transport properties. Efficient strategies for the design and fabrication of heterostructures (*in situ* methods) are discussed, with a focus on the heterostructure formation mechanism. The heterostructure's influence on Na^+ storage and transport properties arises primarily from local distortions of the structure and chemo-mechanical coupling at the phase interface, which may accelerate ion/electron diffusion, create additional active sites, and bolster structural stability. Finally, we offer our perspectives on the existing challenges, knowledge gaps, and opportunities for the advancement of heterostructure engineering as a means to develop practical, high-performance sodium-ion batteries.

* Corresponding author.
E-mail address: clairexiong@boisestate.edu (H. Xiong).
[1] Authors contributed equally.

https://doi.org/10.1016/j.esci.2023.100139
Received 12 October 2022; Received in revised form 3 April 2023; Accepted 28 April 2023
Available online 4 May 2023

1. Introduction

Sodium-ion batteries (SIBs) are promising alternatives to lithium-ion batteries (LIBs) and have received intensive research interest because SIBs have similar electrochemical properties to LIBs and Na is an abundant resource [1,2]. However, when used in SIBs, most existing electrode materials used for LIBs suffer from sluggish kinetics and inferior cycling stability because Na^+ has a larger ionic radius (1.02 Å) than Li^+ (0.76 Å). Developing suitable electrode materials to achieve high-performance SIBs is therefore increasingly important. Through the in-depth study of SIBs, various electrode materials with different reaction mechanisms have been extensively explored as electrode candidates, such as carbon-based materials, transition metal dichalcogenides, p-block elements, layered transition metal oxides, hexacyanoferrates, polyanionic compounds, and organic materials [3–7]. Although the electrochemical performance can be increased to some extent by adjusting the morphology and structure of single-phase materials, it is still difficult to simultaneously achieve high specific capacity, cycling stability, and superior rate capability in single-phase electrode materials. In response to this challenge, the last decade has seen a steady increase in research on electrode materials with multiple phases integrated to form heterostructures (Fig. 1).

A heterostructure is defined by the integration of two or more distinct phases with a shared interface. The integration of these phases generates unique chemistry and physics at the interface, which imbue the electrode with altered properties (Fig. 2). Local distortions of electronic structure generate electric fields that can activate new sites for Na^+ storage and accelerate ion and electron transport. Chemomechanical coupling and microstrain generated by interfacial bonding can bolster the mechanical integrity of otherwise fragile electrode materials. The interfacial phenomena that underly the enhanced electrochemical properties in SIB heterostructures are just beginning to be uncovered. Significant knowledge gaps exist regarding the mechanism of heterostructure formation, limiting current strategies for the intentional design and synthesis of heterostructures. The local interactions at the heterostructure interface have long-range effects, demanding the application of advanced, complementary characterization techniques that span from the atomic scale to the entire cell. Heterostructures are a promising avenue toward a new class of high-performance electrode materials but face numerous challenges compared with their single-phase counterparts. We present recent progress on interface engineering of heterostructured electrode materials for SIBs, with a focus on efficient methods for heterostructure synthesis. We aim to provide a comprehensive perspective on the driving forces for the formation of heterostructures and the mechanistic origin of their altered electrochemical properties.

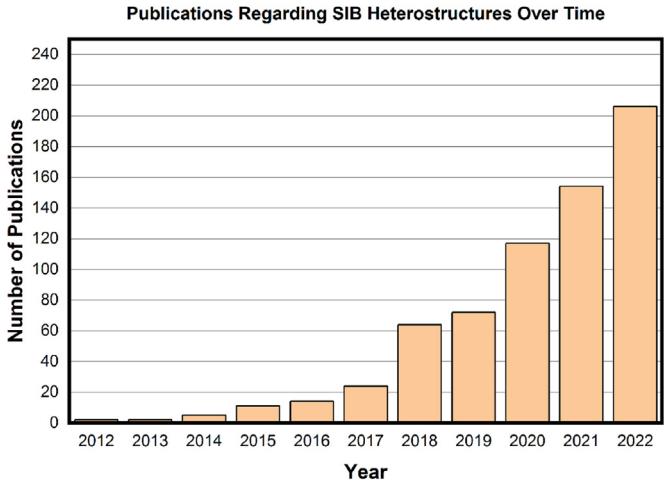

Fig. 1. The number of unique publications over time on sodium-ion battery heterostructures (identified by Web of Science™ search for (ALL=(sodium ion battery)) AND ALL=(heterostruct* OR biphas* OR multiphas* OR triphas* or intergrow*), March 2023.

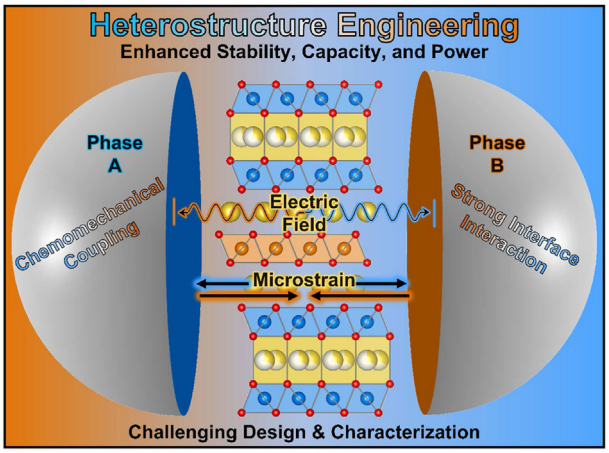

Fig. 2. Schematic illustration of heterostructure materials for SIBs.

2. Heterostructure engineering – design and *in situ* synthesis

Heterostructure engineering can be defined as the rational design and assembly of two or more phases with different chemical composition, specific order (or disorder), and relative orientation of interfaces. The architecture of the heterostructure is defined by the interfacial chemical bonding, geometry, relative amount, and fundamental nature (e.g., composition, structure) of the individual components of the heterostructure. These qualities of the heterostructure largely determine the electrochemical performance. Therefore, the ability to synthesize a well-designed heterostructure with strong interaction between components, controlled defect distribution, and suitable interfacial geometry is vital.

Classification of heterostructures into subgroups depends on the specific variables of interest — chemical composition, crystal structure, dimensionality (0D/1D/2D/3D), morphology, or performance functionality (e.g., positive or negative electrode, ion/electron conduction and/or storage, corrosion protection) may all reasonably be applied to divide related heterostructures into categories.

Synthesis methods for heterostructure preparation can be broadly classified into *ex situ* and *in situ* strategies. An *ex situ* strategy is a multistep material synthesis method that usually involves the synthesis of one material (A) as a substrate and then the introduction of another component (B) on the surface of or mixed with the substrate to construct the heterostructure (A + B → A@B). Coatings are a typical example of *ex situ* synthesis and have been well studied for many classes of electrode materials.

On the other hand, with an *in situ* synthetic strategy, the interfaces of the heterostructure conveniently and efficiently self-assemble as a result of chemical and/or physical processes. The so-called “one-pot” synthesis involving hydrothermal or solvothermal reactions that result in heterostructures is a typical example of *in situ* synthesis. The material properties of heterostructures prepared by an *in situ* strategy can be superior to those of single-phase materials and heterostructures prepared by *ex situ* strategies due to the stronger interaction between the distinct phases. In many cases, a combination of two or more *in situ* and *ex situ* synthesis steps can produce even more complex heterostructures.

Compared with the *ex situ* synthetic strategy, the *in situ* method has the advantage of simultaneously realizing compositional regulation and architectural design. However, understanding the atomic-level mechanisms of *in situ* synthesis and phase interaction that modify the electrode properties is substantially more challenging than with the comparatively simple *ex situ* synthesized heterostructures. Therefore, *in situ* synthesis of heterostructured electrode materials warrants significant attention for future research and is highlighted here.

3. Negative electrode heterostructures

Different heterostructures have been explored as negative electrode materials [8] for SIBs, including carbonaceous materials [9,10], monometallic materials [11,12], bimetallic materials [13], 2D materials (e.g., MXenes/graphene/phosphorene) [14–16], and complex combinations of multiple classes of these materials [17–20]. To provide a concise discussion that covers these various material systems, we refer readers to the referenced reviews and primary literature for detailed comparisons of the synthesis methods. Conversion-type monometallic electrodes (M_aX_b, X = O, S, Se) as potential negative electrode materials for SIBs have been investigated due to their high theoretical capacity and natural abundance. However, the reaction intermediates (e.g., Na_2O, Na_2S, and Na_2Se) generated from the conversion reaction are reactive with the electrolyte, forming an undesirable solid–electrolyte interphase (SEI) on the surface of the electrode material that may strongly hinder the reversibility of the conversion reaction. In addition, the large volume expansion and contraction during charging and discharging can lead to pulverization and deterioration of the active materials. Fabricating heterostructured negative electrode materials could offer additional opportunities for delivering better Na^+ storage performance by providing the unique properties of a stable SEI, a confined electrochemical reaction space, and interfacial storage capacity. These advantages have driven researchers to explore suitable methods for synthesizing heterostructured negative electrode materials for efficient Na^+ storage.

3.1. *In situ synthesis strategy and mechanism of heterostructure formation*

Solvothermal/hydrothermal process are widely used one-pot methods to prepare various heterostructure electrode materials. Typically, the different precursors are mixed uniformly and held under high temperature and pressure inside the reaction vessel where they can react to form solid products with unique, spontaneously formed nanostructures. As a result of atomic-level interactions, the heterostructure electrodes produced by the solvothermal/hydrothermal method often exhibit active edges/defects and high specific surface areas. The 2D/2D heterostructure of transition metal dichalcogenides (TMDs), consisting of nanosheets, is readily synthesized using *in situ* hydrothermal/solvothermal methods [14,17,21–24]. Transition metal precursors, such as Na_2MoO_4, $(NH_4)_2MoS_4$, $SnCl_4$, K_2 $(Sn(OH)_6)$, and WCl_6 [14,17,21–24], react with water-soluble sulfur sources such as CH_4N_2S and C_2H_5NS that can also serve as reducing agents. The hydrothermal and solvothermal processes are highly scalable, which is attractive for practical applications.

Partial reaction (e.g., carbonization, sulfurization, or selenation) has also attracted major attention for the *in situ* preparation of heterostructured electrode material [9,10,25,26]. Generally, the precursor can be partially reduced to another material when annealed under an appropriate gas atmosphere, such as Fe_3O_4 to FeS via a sulfurization process (Fig. 3) [12]. The proportions of the components can be controlled by adjusting the annealing temperature, time, and atmosphere concentration. During the annealing process, the metal reacts to form into different materials because of their different formation energies, promoting the *in situ* synthesis of atomically integrated heterostructures. Although the self-assembly method demonstrates intriguing potential for fabricating heterostructures, it is difficult to precisely control the exposed lattice planes that influence the electrode properties. Hence, it remains a fundamental research challenge to develop the synthetic techniques to achieve both controllable and scalable features.

3.2. *Mechanisms of interface interaction*

Interface engineering through the controlled fabrication of heterostructures has exhibited unique advantages for energy storage and conversion due to a variety of synergistic effects. For instance, the heterostructure can combine the merits of its different components to overcome the shortcomings of a single phase, which provides a promising way to enhance the electrochemical performance of individual electrode materials. Additionally, heterointerface engineering has the key effect of improving the electronic and ionic conductivity, which can reduce the polarization and take full advantage of electrode materials in rapid charge/discharge processes. Recently reported single-phase negative electrode materials, such as metal oxides, metal sulfides, and black phosphorus, are semiconductors with intrinsically wide band gaps [18,27–29]. Building a heterostructure can optimize the band structure of the heterostructured electrode materials due to unique interactions at the heterointerface, thus enhancing the conductivity. Moreover, the interfacial coupling effect can facilitate charge redistribution that will accelerate ion/electron transport and create more active sites, thereby enhancing the reversible capacity and rate capability.

3.2.1. *Built-in electric field accelerating charge transport*

The effect of a heterointerface on electrochemical performance is strongly related to the particular heterostructure. To achieve better

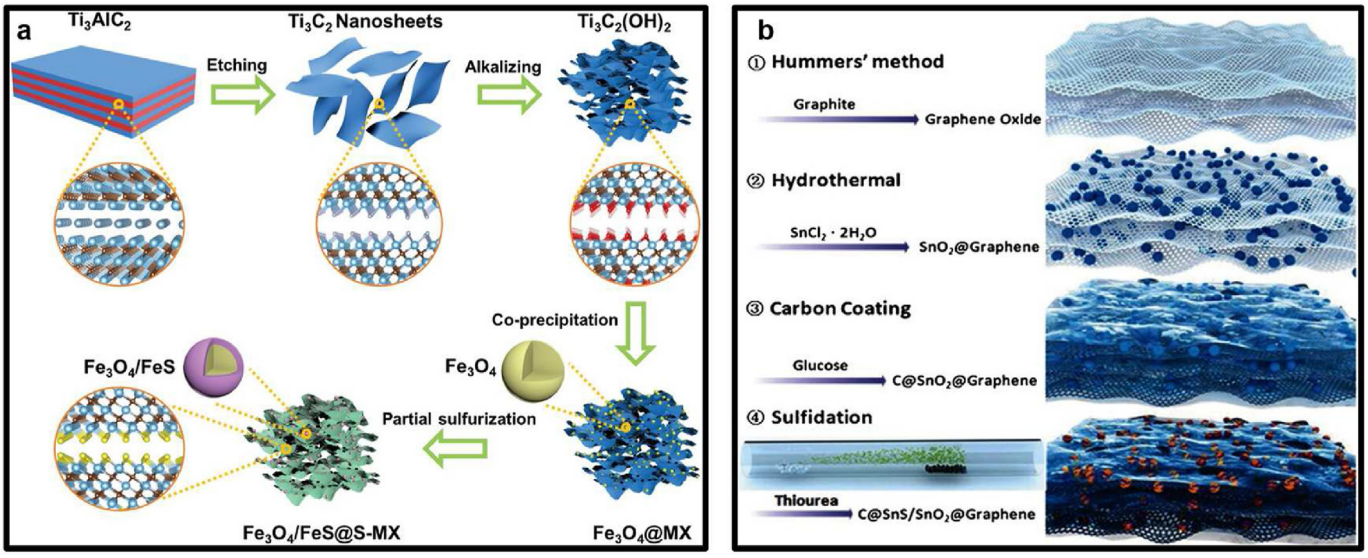

Fig. 3. Schematic illustration of heterostructure preparation. (a) Fe_3O_4/FeS samples [12]. Copyright 2020, Wiley. (b) C@SnS/SnO_2@Gr architecture [11]. Copyright 2016, Wiley.

performance, it is necessary to construct a hybrid with a unique interface. Once the two substances with different band gaps come into contact, the charge will redistribute at the heterointerface spontaneously until the Fermi levels achieve a balance. As a result, the negative charges will accumulate on the lower Fermi level side and positive charges on the higher Fermi level side, forming a built-in electric field. Driven by this built-in electric field, ion diffusion and charge transfer will be accelerated. Additionally, built-in potential caused by the accumulated electrons and holes around the heterointerface could endow the materials with high conductivity.

The specific role of the heterointerface in sodium storage has been investigated using a combination of experimentation and density functional theory. Guo *et al.* have successfully constructed monometallic SnS/SnO_2 heterostructures with the same metal and different non-metal elements to investigate the charge-transfer effect in SIBs (Fig. 4) [11]. During the discharging process, the built-in field formed at the heterointerface will point to the narrow-band-gap side (p-type, SnS) from the wide band gap side (n-type, SnO_2). Under this condition, the charge distribution at the heterointerface will be broken, which could contribute to a low Na^+ diffusion barrier on the SnO_2 side and yielding fast charge-transfer kinetics. Accompanied by the charge balance, the built-in electric field will vanish. But Na^+ transport can still occur at the heterointerface, driven by the concentration gradient to realize excellent reaction kinetics.

Heterostructures constructed using the same non-metal element and different metal elements have also been explored and demonstrated high reversibility based on the strength of the build-in electric field. For example, Ma *et al.* synthesized a bimetallic FeP/CoP heterostructure to investigate the reaction kinetics in Na^+ storage [13]. The direction of the electric field formed at the heterointerface pointed to FeP from CoP, which induced electrons to move from CoP to FeP. Consequently, the Na^+ adsorbed on the FeP side due to electrostatic interaction, inducing an inverse electric field that enhanced Na^+ diffusion during charge/discharge. At the same time, it is important to note that the heterointerface location in a composite can also affect the Na^+ storage properties. In layer-to-layer 2D heterostructures such as black phosphorus/graphite (or few-layer phosphorene/graphene) [30–32] or MoS_2/graphite [21,33], a larger contact area can promote more effective charge distribution between the 2D layers and enable tuning for a larger range of electronic structures, thus facilitating the reaction of molecules on the 2D surface [15]. When it comes to a core–shell structure or a blended structure, the heterointerface and active surfaces are largely buried, which can make it more difficult for the ions to overcome the diffusion barriers and access the heterointerface, resulting in inferior reaction kinetics [19].

3.2.2. *Built-in electric field generating Na^+ adsorption sites*

In addition to enhancing the kinetics, the interfaces of heterostructures can form active sites, which can improve the Na^+ storage capacity. Electron redistribution at the interface allows extra Na^+ to be adsorbed at the negatively charged sites, contributing to a higher specific capacity. Stronger adsorption energy can be acquired at the heterostructure interface than with single-phase materials, allowing Na^+ ions to adsorb more easily and resulting in higher reversible specific capacity. To clarify the synergistic effect of Na^+ storage on enhancing the capacity, a MoS_2@MoO_2–C hetero-nanostructure was constructed by Xiong and coworkers [20], who found that its adsorption energy was stronger than that of MoS_2 and MoO_2 on their own. The enhanced adsorption energy of Na^+ ions was proposed to arise from the redistribution of electrons at heterointerfaces. The built-in electronic field accumulated negative charges on the MoS_2 side and positive charges on the MoO_2 side, creating a charge transport pathway from MoO_2 to MoS_2 (Fig. 5a). Furthermore, the Na^+ was attracted to the MoS_2 surface, neutralizing the accumulated electrons and increasing the capacity. A "job-sharing" mechanism in LIBs was proposed by Jamink and Maier to explain the extra Li^+ storage at interfaces [35]. To determine whether the mechanism remains valid for Na^+ storage, Xiong *et al.* studied the Na^+ storage behavior of heterostructure interfaces via solid state nuclear magnetic resonance (NMR) [34]. The lattice mismatch between different crystals in the heterostructure can promote defects near the interface, which can act as active sites to store Na^+. They quantitatively interrogated this by solid-state NMR for individual carbonaceous TiO_2, MoO_2, and carbonaceous TiO_2/MoO_2 heterostructures. Na^+ not only was observed in TiO_2 and MoO_2 materials but also resided at the interfaces between MoO_2 and TiO_2 (Fig. 5b). Quantitative analysis results demonstrated that the heterointerface contributed up to 20% capacity.

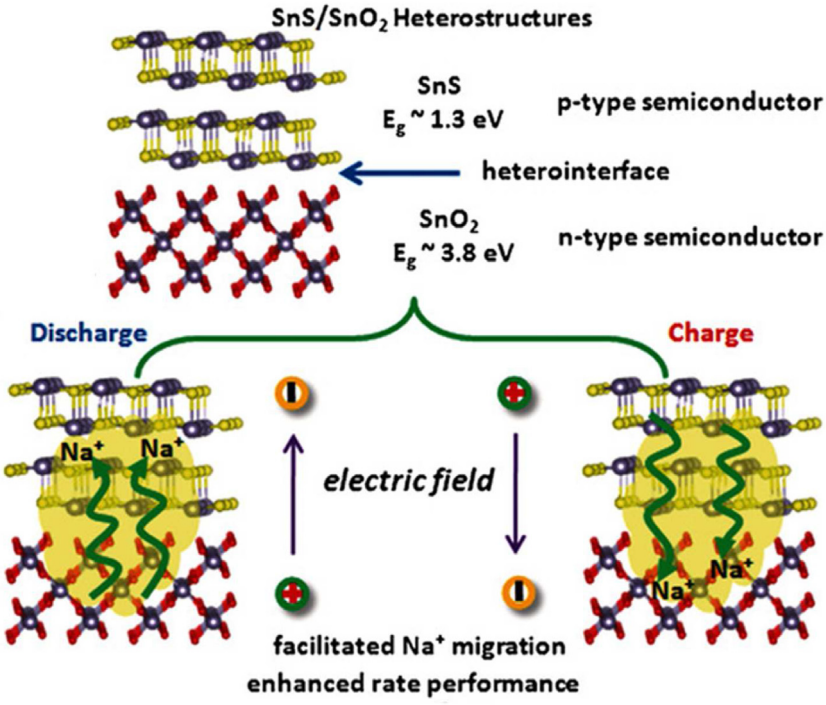

Fig. 4. Schematic illustration of enhanced high-rate capacity mechanism of SnS/SnO_2 heterostructure [11]. Copyright 2016, Wiley.

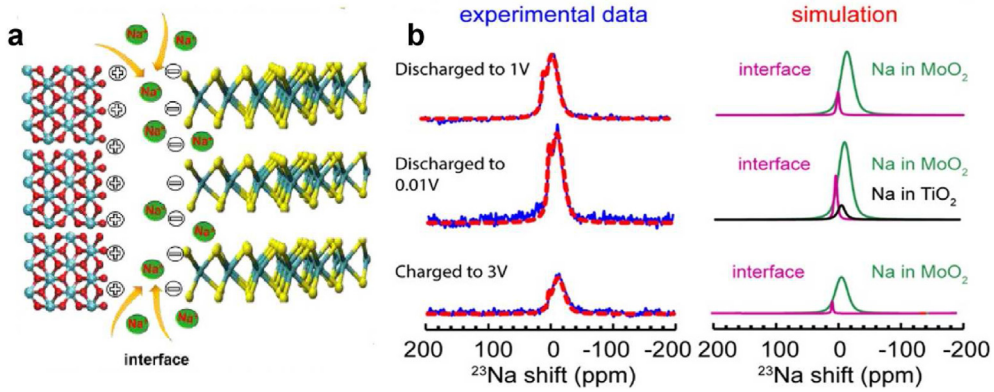

Fig. 5. (a) Schematic illustration of active sites induced by charge redistribution [20]. Copyright 2020, Royal Society of Chemistry. (b) Experimental and simulated ^{23}Na NMR spectra of TiO_2@ MoO_2 electrodes at different states of charge [34]. Reprinted (adapted) with permission. Copyright 2018, American Chemical Society.

3.2.3. *Morphologically controlled chemomechanical strain*

High-capacity conversion-type electrode materials have attracted significant attention as potential negative electrode candidates for SIBs due to their high theoretical capacity, but the severe mechanical degradation induced by huge volume expansion severely limits their practical application [37]. Promising morphologically controlled heterostructures have been reported to effectively relieve the stress caused by the volume change. A cross-linked stacking architecture can help to transmit additional force from the point of load to its surroundings [38]. Thus, the entire arrangement of this heterostructure can be more robust than that of a hierarchical structure. Utilizing this concept, Wu *et al.* designed and prepared a "bird's nest" layered heterostructure $(SnFe)S_2$ [36]. Assisted by finite element method (FEM) simulation, the structural self-evolution of stress distribution of $(SnFe)S_2$ and pure SnS_2 were compared (Fig. 6). The electric field intensity of $(SnFe)S_2$ was evenly distributed as the folding structure increased, showing a homogeneous distribution of stress. However, for the pure SnS_2 structure, the electric field became non-homogeneous with increasing current, indicating a progressively greater stress concentration. The evolution of negative electrode heterostructures in response to cycling is of significant concern. Structural and surface changes that result from sodiation may or may not be reversible upon desodiation [39,40]. Therefore, it is important to investigate the heterostructure not only in its pristine state but also after exposure to real operating conditions in order to develop a complete picture of electrode behavior.

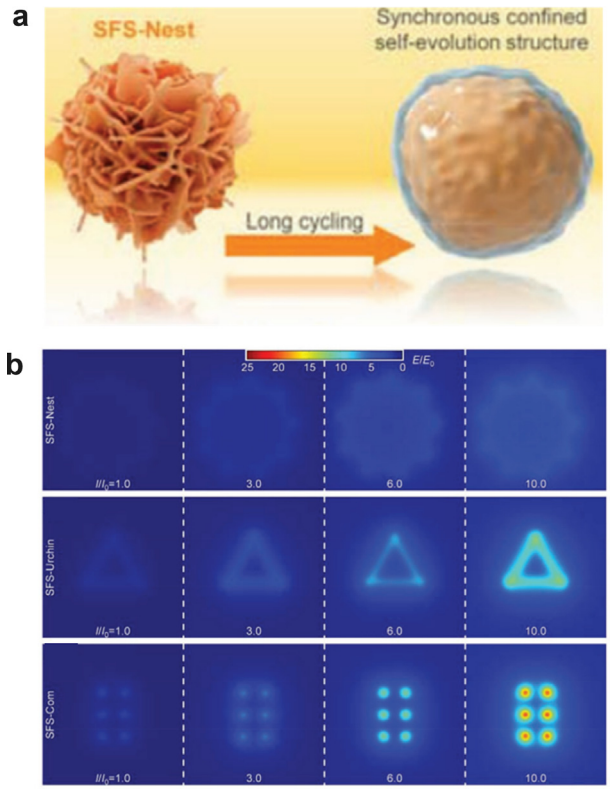

Fig. 6. (a) Schematic of nest-like heterostructure. (b) FEM simulations of different heterostructures to engineer stress distribution [36]. Copyright 2022, Wiley.

4. Positive electrode heterostructures

Among the various classes of positive electrode materials for SIBs, layered transition metal oxides (LTMOs) are attractive compared to polyanionic compounds [41], NASICON [42,43] structures, and Prussian blue analogues [44] because LTMOs have a higher energy density [45] and utilize abundant elements. While the benefits of heterostructures have been demonstrated in all of these positive electrode systems [46–49], LTMOs (and closely related spinel-type oxides [50]) display unique *in situ* heterostructure formation without the significant inclusion of carbon or the advanced *ex situ* synthesis methods usually required in other material systems [51]. However, further investigation into LTMO heterostructure (layered–layered and layered–spinel structures) formation and interaction mechanisms is needed to fully realize their benefits.

LTMOs are classified according to the notation proposed by Delmas [52], with a letter describing the sodium site geometry (O – octahedral, P – prismatic) and a number indicating the layers (e.g., 1, 2, 3, 4, 6) required to achieve translational symmetry along the layering direction. A prime symbol (′) is often used to denote a distorted version of a given structure, such as monoclinic (C2/m) O′3 $NaNiO_2$ compared to rhombohedral (R-3m) O3 $NaFeO_2$. The most commonly observed forms of LTMOs in their pristine state (before charge/discharge) are the O3, P2, and P3 structures (Fig. 7).

In the case of heterostructured LTMOs, combinations of these and other structures can be integrated at the atomic level through *in situ* synthesis methods [51]. While many examples of LTMO heterostructures have been reported, there has been relatively little discussion in the literature regarding design strategy and the associated mechanism of heterostructure formation, or the mechanism of the phase interface's influence on electrochemical properties. A layered heterostructure can significantly enhance the electrochemical properties by combining the fast transport of *P*-type phases with the high storage capacity of O-type phases. The heterostructure induces chemomechanical coupling at the phase interface, which can mitigate the mechanical stress that occurs during cycling. Substantial opportunity exists for future research to understand these mechanisms, which could lead to significant advancement in our ability to control the properties of LTMO-based electrodes.

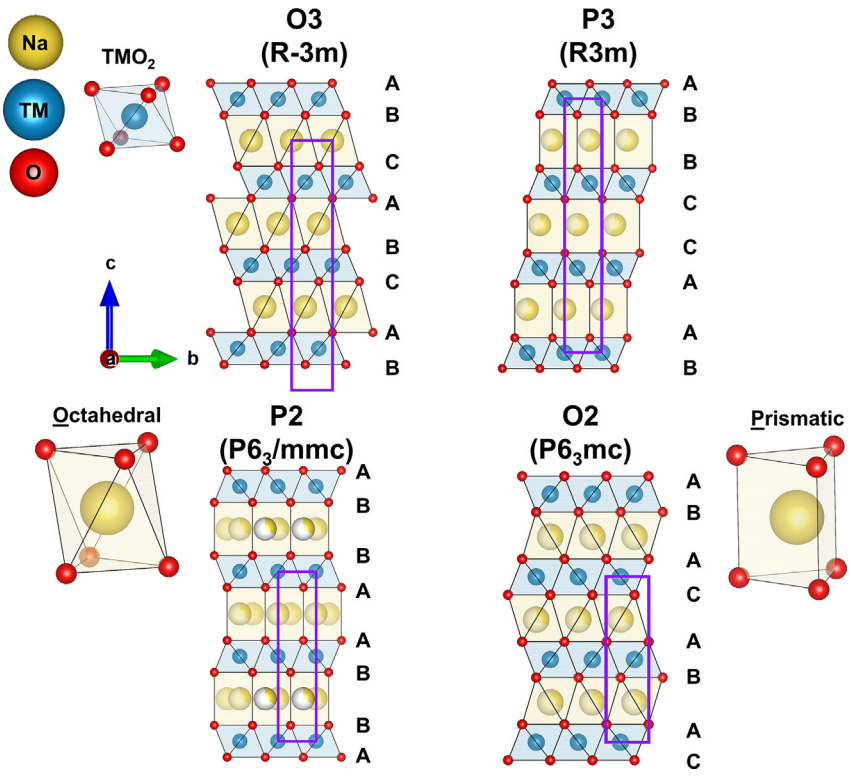

Fig. 7. The common LTMO structures, with purple lines indicating the unit cells. Reproduced from Ref. [51] with permission under a Creative Commons Attribution 4.0 International Public License.

4.1. Synthesis strategy and mechanism of heterostructure formation

Heterostructured positive electrodes based on LTMOs have generally been prepared by one of two primary routes: manipulation of the solid-state reaction conditions (temperature, quenching), or manipulation of the composition (transition metal composition, sodium content, and/or dopants). Amine *et al.* utilized *in situ* synchrotron high-energy XRD (HEXRD) to monitor the structural evolution of $Na_xNi_{1/3}Co_{1/3}Mn_{1/3}O_2$ during high-temperature synthesis to elucidate the temperatures at which phase transitions occurred (Figs. 8a and b) [53]. By controlling the calcination temperature and quenching process, they were able to create three materials with distinct phases — a triple phase P2/O3/O1, a binary phase P2/O3, and a P2/P3 phase (Fig. 8c). As a result of their varied heterostructures, all three electrodes displayed vastly different electrochemical, thermal, and interfacial properties, despite having the same overall composition. Understanding the reaction pathway between the precursors and final product can therefore allow for heterogeneous, metastable intermediate phases to be captured. *In situ* characterization techniques that interrogate structural evolution during synthesis are therefore highly valuable toward the design of heterostructured LTMO electrode materials.

In single-phase LTMOs, O3 type phases typically form for compositions with high sodium content (Na_xTMO_2, x ~ 0.8–1.0) and large-radius, low-valence transition metal elements (e.g., Ni^{2+}, Fe^{3+}), while P phases occur for low sodium content (x < 0.8) paired with small, high-valence transition metals (e.g., Mn^{4+}) [54]. Chen *et al.* demonstrated that variation in the sodium content in $Na_{0.9-x}Ni_{0.45}Mn_{0.55}O_2$ resulted in the transition from a pure O3 phase to a biphasic O3/P2 intergrowth composite when $x = 0.02$, with the resulting superior capacity retention (71.1% after 250 cycles vs. 38.3%), lower interfacial resistance, and increased structural stability most likely arising from the intergrown heterostructure [55]. However, additional sodium deficiency resulted in the formation of a NiO type impurity, probably because Ni^{3+} formation was unfavorable. The cation charge balance against O_2^{4-} and the oxidation states of the transition metal elements must be carefully considered to achieve the intended heterostructure design and avoid impurity formation. Zhou *et al.* demonstrated a biphasic O′3/P2@spinel heterostructure with a spontaneously formed spinel-like titanium oxide segregated on the surface, $NaMn_{0.8}Ti_{0.1}Ni_{0.1}O_2$, which enhanced the chemical, electrochemical, and thermal stability compared to homogeneous O′3 $NaMnO_2$ [56]. The spontaneous segregation of one species on the surface is common in oxides but has rarely been reported in SIB materials and deserves significant additional study. The influence of composition in $Na_{1-x}Ni_{1-y}Mn_yO_2$ was systematically studied by Xiao *et al.* [57]. Systematic analysis of different Ni:Mn ratios elucidated that higher Mn content promoted the P2 structure, and intergrown O3/P2 heterostructures only occurred in a narrow composition range. O3/P2-type $Na_{0.85}Ni_{0.4}Mn_{0.6}O_2$ material could have the O3/P2 ratio tuned by substituting Mn for other TMs. While the $Na_{0.85}Ni_{0.4}Mn_{0.6}O_2$ material would form an 87%/13% P2/O3 structure, substitutions of Mn with 0.1 Fe, Co, or Ti led to a decreased phase fraction of P2, with P2 contents of 12.3, 7.9, and 0%, respectively. The phase fractions correlated strongly with the ionic potential [54,57] of the TMs, suggesting the usefulness of compositional variables (i.e., ionic potential) to design the phase ratio in heterostructured LTMO positive electrodes. Given the influence of TM composition on structure, heterostructures utilizing composition gradients (via coprecipitation), such as those well-studied in lithium-based LTMOs, have rarely been studied in SIBs and could be another valuable avenue to develop heterostructured LTMO electrodes.

While a number of studies identify factors that promote the formation of LTMO heterostructures, there are significant gaps in the understanding of *how* LTMO heterostructures form. For example, a secondary O3 phase could grow from nucleation sites within the bulk of a primary P2 phase as sodium is intercalated in increasing amounts while the calcination progresses. Alternatively, the O3 phase could gradually form starting from the surface, consuming the P2 phase and sodium as it grows toward the bulk of the particle. Other plausible scenarios could be considered, but there is little to no evidence in the existing literature to support any

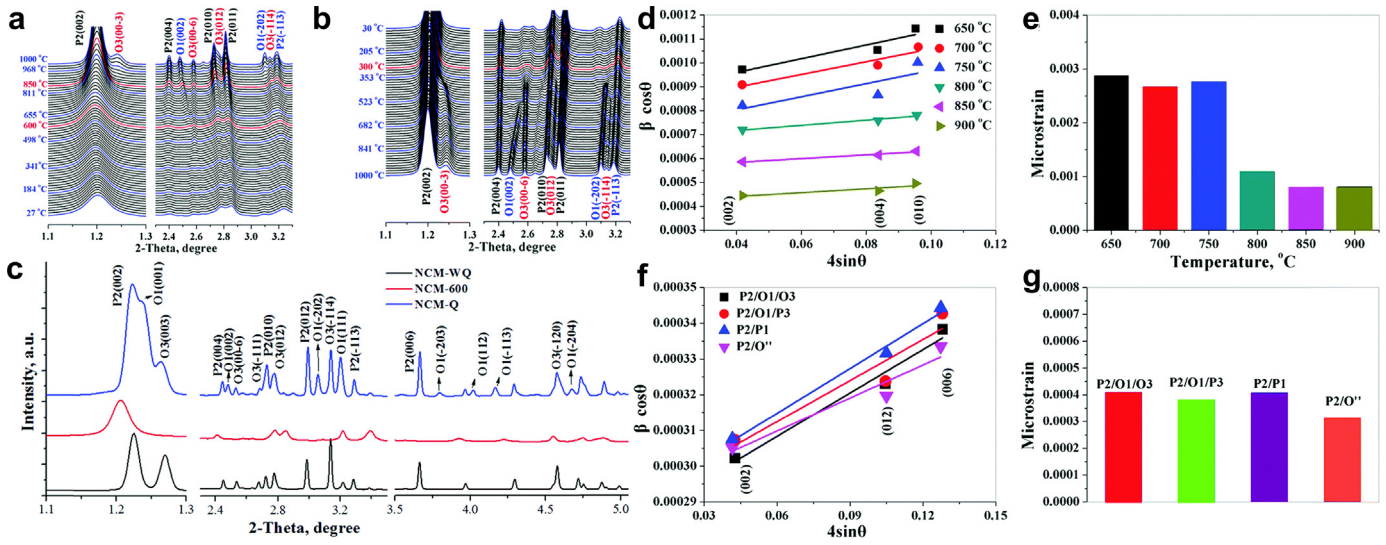

Fig. 8. (a, b) *In situ* XRD of the $Na_xNi_{1/3}Mn_{1/3}Co_{1/3}O_2$ material during heating and cooling, respectively. (c) *Ex situ* XRD of $Na_xNi_{1/3}Mn_{1/3}Co_{1/3}O_2$ samples prepared at different calcination procedures. (d, e) Williamson–Hall analysis of microstrain during calcination and (f, g) during electrochemical cycling. Copyright 2017, Royal Society of Chemistry [53].

specific hypotheses on the heterostructure formation mechanism. How to differentiate between heterostructures formed via kinetically constrained processes (such as anisotropic and/or incomplete reactions and quenching) and those formed from thermodynamically favorable processes is also generally uncertain. LTMO heterostructures are often shown to be integrated along the layering direction, but in some cases they appear to be joined at the edges of the layers [58,59]. This difference in heterostructure geometry could arise from a different mechanism and result in different properties. Other than the relative phase ratio, factors such as the domain size between phase interfaces may be important for the resulting properties of the electrode. These unanswered questions necessitate the application of both local and long-range *in situ* characterization techniques (e.g., transmission electron microscopy and X-ray diffraction) to support the development of theoretical models of LTMO heterostructure formation.

4.2. *Mechanisms of interface interaction*

Positive electrode materials can also benefit from the built-in electric field and morphological optimizations seen in negative electrode materials. However, the distinctive chemistry of LTMO systems compared to those of negative electrode materials can bring about unique mechanisms of heterostructure interface interaction that we highlight in this discussion. The bonded phase interface between different layered structures generates a direct link for the exchange of mechanical forces caused by electrochemical reactions within each phase and intertwines their Na^+ transport mechanism.

4.2.1. *Integrated Na^+ transport mechanisms enhance diffusion*

As a result of the different sodium site geometries, *P*- and O-type phases tend to demonstrate significant differences in the Na^+ diffusion. In prismatic phases, the Na^+ ion diffuses easily between face-sharing prismatic sites. Octahedral phases require that Na^+ move through intermediate tetrahedral sites, which presents a higher energy barrier compared to the diffusion mechanism in *P*-type structures. Consequently, *P*-phases typically have significantly better performance at a high rate. However, since *P*-phases are usually sodium deficient, there is a tradeoff between theoretical capacity and rate capability when choosing between single-phase materials.

In contrast, heterostructures can combine *P*-phase(s) to allow fast Na^+ transport with O phase(s) that act as a high-capacity reservoir for Na^+ ion storage [60,61]. Further, the *P*-phase can act as a highway for Na^+ ions to reach the core of secondary particles, mitigating nonhomogeneous reactions between the surface and bulk of secondary particles that could generate significant stress. Consequently, the exact nature of the grain size distribution of each phase, the relative orientation and location of the grains, and the secondary particle size can also have a significant effect on Na^+ transport and overall structural stability. For example, a larger O-type grain will have a longer diffusion length to its core, requiring more time to fully (de)sodiate than a smaller O-type grain. Layered phases stacked on top of one another will have a less direct path for Na^+ transport than those aligned at the edges, where diffusion can occur directly. The possibility of individual phases being enriched in certain elements can further complicate the investigation of these heterostructures. Therefore, probes that can access grain size, orientation, and composition with high spatial resolution are extremely valuable but have rarely been applied in previous studies of LTMO heterostructures. We have previously reviewed these and other aspects of LTMO heterostructures in detail [51].

Several LTMO heterostructures have exhibited considerably improved Na^+ transport and storage properties compared to single-phase materials. Guo *et al.* demonstrated an order of magnitude increase in the Na^+ diffusion coefficient of a O3/P3 heterostructure compared to a single-phase O3 material [60]. Lee *et al.* showed that an O3/P2 heterostructure could retain 95% of its capacity at 150 mA/g compared to the capacity at a low rate, while the single-phase O3 material retained only 60% under the same conditions [61]. The O3/P2@spinel heterostructure prepared by Zhou *et al.* [56]. Took advantage of this O3/P2 synergy in combination with the lower interfacial resistance of a three-dimensional, spinel-like surface layer with high electronic and ionic conductivity. Heterostructures based on combinations of P2 and P3 phases have also been demonstrated. The sodium site geometry is prismatic in both P2 and P3 phases, so influence of the interface on the mechanism of Na^+ transport is more subtle than in the case of O3/P3 or O3/P2 heterostructures. In the $Na_{0.67}Mn_xCo_yAl_zO_2$ system, a P2/P3 heterostructure was identified to have the best performance at high rate compared to pure P2 or P3 materials [62]. The $Na_{0.78}Cu_{0.33-x}Zn_xMn_{0.67}O_2$ system demonstrated superior rate performance with its Zn-exchanged P2/P3 heterostructure compared to a P2 structure at $x = 0$ [63]. The superior rate performance of this heterostructure is surprising, considering that Zn doping induced Na^+/vacancy ordering, which is usually cited as a cause of poor kinetics

[64]. In contrast, in the $Na_xNi_{0.22}Co_{0.11}Mn_{0.66}$ system, the P2 phase was found to have higher capacity at high rate compared to a P3 structure and a P2/P3 heterostructure [65]. These contrasting reports indicate that in some cases, heterostructured materials are not necessarily guaranteed to provide performance improvements. Triphasic or higher-order phase combinations will necessarily be even more complex to interpret. Further systematic study is needed to identify additional factors that dictate the Na^+ transport properties in heterostructures, especially in P2/P3 systems.

4.2.2. *Chemomechanical interface coupling provides structural reinforcement*

It is regularly observed in single-phase LTMOs that during desodiation, the in-plane lattice parameter (*a*) contracts, the interlayer spacing (proportional to *c*) increases due to oxidation of the transition metals (reducing their radii), and the oxygen repulsion between layers becomes stronger because the screening effect from the positively charged Na^+ ions is reduced [7]. This structural distortion often triggers phase transitions associated with gliding of the TMO_2 layers without TM-O bond breakage, as well as Na^+ rearrangement to reduce the interlayer repulsion. In single-phase materials, there is nothing to prevent this lattice distortion and phase transformation, apart from other nearby particles mechanically restricting the distortion. Accumulated stress from this distortion may eventually cause secondary electrode particles to crack, increasing the surface area for electrolyte decomposition or loss of contact with conductive pathways that allow Na^+/electron transport.

In contrast, heterostructured LTMOs will experience the coupling of lattice distortion in one phase to its intergrown neighbors. The distinct phases will not undergo identical degrees of contraction/expansion at all potentials, resulting in a "pinning" effect. For one phase to contract or expand, it must "pull" on the intergrown phase, like reinforcement bars in concrete. As a result, phase transitions that might occur for single-phase materials can be restricted by chemomechanical coupling with the heterostructure. There may also be significant microstrain at the interface due to lattice mismatch, even in a pristine material. This microstrain could further contribute to the pinning effect and mitigate the development of further microstrain by "prestressing" the phases near the interface. Recently, Wei *et al.* studied the effect of interfacial stress generated by lattice mismatch at P2/Li–O3 biphasic heterointerfaces [66]. High-angle annular dark-field scanning transmission electron microscopy (HAADF-STEM, Figs. 9a and b) was used in combination with geometric phase analysis (GPA) to examine the local strain field near the phase interface (Figs. 9c and d). Complex phase transition could be effectively inhibited by interfacial shear stress, with the Li–O3 phase restricting in-plane contraction and TMO_2 layer gliding in the P2 phase.

We note that the distinction between intergrowth heterostructures and stacking fault(s) is blurred when the number of sequential layers with unique stacking sequences approaches the number of layers in a single unit cell. The P2/Li–O3 material (Figs. 9a and b) contains regions where only 1–3 layers deviate from the ideal P2 stacking sequence; an argument could be made that these are perhaps more accurately categorized as individual or clustered stacking faults than a heterostructure. The local information given by scanning transmission electron microscopy (STEM) does not capture the long-range average features of the heterostructure unless a large number of particles are observed. For coherently layered structures containing stacking faults, the X-ray, neutron, and electron diffraction patterns for statistically distributed stacking sequences can be simulated and fitted using software such as DIFFaX [67] and FAULTS [68]. These simulations have been successfully applied to layered oxides to understand phase transformations during synthesis and electrochemical cycling [69,70]. Treatment of the diffraction data in this manner, in combination with local analysis via microscopy, is recommended to describe more completely the nature of the heterostructure, which may contain very small domains (1–3 layers) as well as coherently layered domains sufficiently large to generate distinct peaks in the diffraction pattern. Williamson–Hall analysis [71] of the diffraction pattern can also provide information about the domain size and microstrain in each phase. This analysis method was successfully applied by Amine *et al.* (Figs. 8d–g) [53] to support that the superior stability of triphasic P2/O3/O1 $Na_xNi_{1/3}Co_{1/3}Mn_{1/3}O_2$ possibly arose from the lack of microstrain increase after charging, due to the presence of

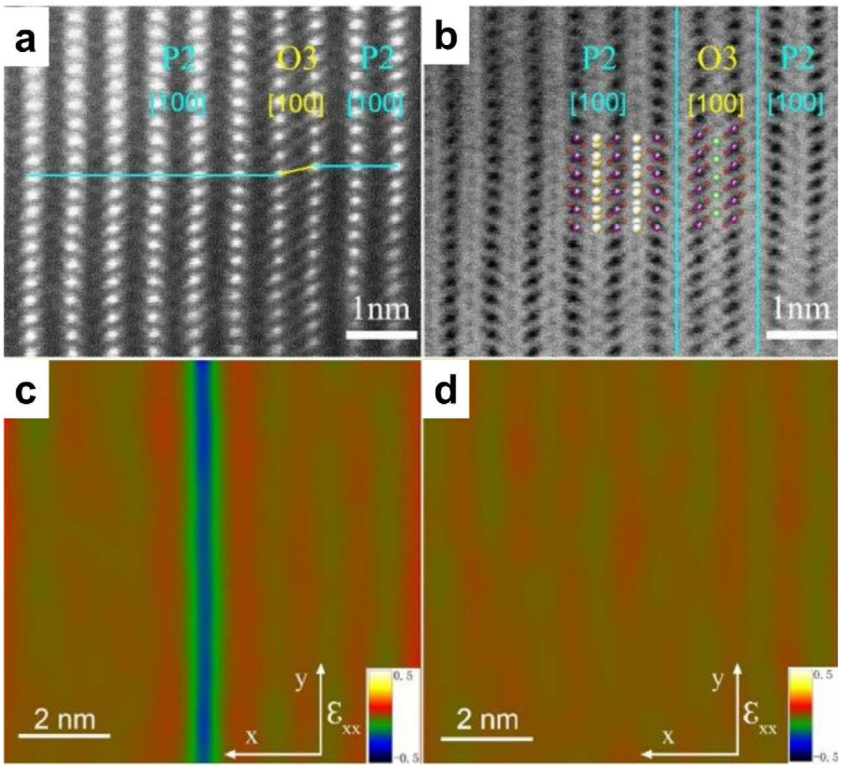

Fig. 9. (a, b) STEM and (c, d) GPA of NaLiMNO, showing the strain field associated with the O3/P2 phase interface [66]. Copyright 2021, Elsevier.

heterostructure interfaces. The domain size information from Williamson–Hall analysis could also indirectly grant insight into the dynamics of grain growth (through domain size) during the synthesis process.

5. Summary

Heterostructures present the possibility of significantly enhancing the properties of electrode materials, but they introduce substantial challenges for design, synthesis, and characterization. *In situ* synthesis techniques whereby heterostructures form spontaneously are an efficient means to prepare this class of electrode materials. However, the currently incomplete understanding of the chemical and physical processes that prompt heterostructure formation limits the ability to design a phase interface with specific desirable properties. When the heterostructure can be prepared with strong interfacial interaction between phases, the local properties of each phase are distorted, which has long-range consequences. The electric field developed by the phase interface can generate additional sites for Na^+ storage and accelerate charge transport. Superior transport properties both in an individual phase and at the interface in the heterostructure can mitigate stress development in neighboring phases by reducing the tendency toward anisotropic reaction across the scale of the electrode particles. Additionally, bonding between the phases generates a mechanical link that allows forces caused by electrochemical reactions to be exchanged, bolstering the electrode particles' mechanical integrity. Microstrain associated with lattice mismatching can mitigate the development of excessive strain during electrochemical operation, further stabilizing the electrode. Unveiling the mechanism of interface formation during synthesis, and the heterostructure's influence on the electrode properties, requires a careful combination of local probes and complementary methods that simultaneously capture the long-range changes [72]. Correlating the properties and behavior of the electrode across multiple length scales is necessary to fully understand the influence of the heterostructure.

6. Outlook

Although great advances have been made, the design, synthesis, and comprehension of the synergistic mechanism of heterostructure interfaces in SIBs remains elusive. Heterostructure design ideally allows control over the properties of the distinct phase components, in addition to the nature of their shared interface. In practice, the available synthesis methods lack precise control over many variables of interest. Phase fractions and overall composition are often readily manipulated by the choice of chemistry, but geometric constraints between phases that are harder to control could prevent the maximum benefit of the heterostructure from being realized. If the interfacial contact area is small, then few active sites can be generated, and the built-in electric field may appear only sparsely throughout the heterostructure. Excessive lattice mismatching or other unfavorable surface chemistry between the exposed facets of each phase could reduce the strength of the interface bonding, decoupling the phases and losing the chemomechanical coupling or other interface effects that the heterostructure is intended to promote. The degree of synthetic control over the geometric factors and surface chemistry that dictate the overall strength of the interface interactions is limited and demands significant attention. The system-specific nature of these factors compounds the difficulty of heterostructure design. Therefore, synthetic approaches for heterostructure control that can be generalized across material systems could be extremely valuable and are sorely needed. Beyond these challenges in design and synthesis, the characterization of heterostructures is a pervasive issue that must be addressed to achieve their further development.

Many studies of heterostructured materials have focused on theoretical simulation, and others have implemented powerful experimental characterizations, but rarely have both approaches been applied to interrogate the local behavior at the interface simultaneously with investigation of processes up to the electrode scale. Experimental identification of key parameters that describe the heterostructure — phase ratio, relative domain size, spatial configuration, and interface chemistry and interaction strength — is extremely challenging and demands a variety of complementary spatially resolved and chemically sensitive methods. However, these essential properties of heterostructures have rarely been experimentally probed systematically across a wide range of length scales. Investigation of heterostructure synthesis processes as they occur (*in situ*) is a relatively unexplored avenue that may provide a wealth of information about the mechanisms of heterostructure formation. Simulation efforts also must undertake the challenging endeavor of explaining heterostructure formation and electrochemical behavior from the atomic scale to the electrode scale. To this end, continuous efforts are needed to combine precise theoretical calculations with systematic, multiscale experimental characterization technologies to develop a deeper understanding of the synergistic effect of interfaces in heterostructured electrodes.

In his *Metaphysics*, Aristotle wrote: “In the case of all things which have several parts and in which the totality is not, as it were, a mere heap, but the whole is something beside the parts, there is a cause; for even in bodies contact is the cause of unity …” Though he was referring to a different subject matter, the analogy to heterostructured materials is apparent. The emergent properties of the heterostructure as a whole arise from the interaction of its united but distinct parts (phases). Control over the unique parts of heterostructures and the manner of their unification will remain an attractive avenue toward high-performance electrode materials for sodium-ion batteries.

Declaration of competing interest

The authors declare that they have no known competing financial interests or personal relationships that could have appeared to influence the work reported in this paper.

Acknowledgements

The authors (E. Gabriel, K. Graff, A. Conrado, D. Hou and H. Xiong) acknowledge the support by the U.S. Department of Energy, Office of Science, Office of Basic Energy Sciences program under Award Number DE-SC0019121. E. Gabriel also thanks the U.S. Department of Energy, the Office of Workforce Development for Teachers and Scientists, Office of Science Graduate Student Research (SCGSR) (DE-SC0014664). The funding sources had no direct role in the preparation of the paper or decision to submit the paper for publication.

References

[1] J. Song, B. Xiao, Y. Lin, K. Xu, X. Li, Interphases in sodium-ion batteries, Adv. Energy Mater. 8 (2018) 1703082.
[2] C. Delmas, Sodium and sodium-ion batteries: 50 years of research, Adv. Energy Mater. 8 (2018) 1703137.
[3] X. Zhong, Y. Wu, S. Zeng, Y. Yu, Carbon and carbon hybrid materials as anodes for sodium-ion batteries, Chem. Asian J. 13 (2018) 1248–1265.
[4] L. Li, Y. Zheng, S. Zhang, J. Yang, Z. Shao, Z. Guo, Recent progress on sodium ion batteries: potential high-performance anodes, Energy Environ. Sci. 11 (2018) 2310–2340.
[5] L. Fang, N. Bahlawane, W. Sun, H. Pan, B.B. Xu, M. Yan, Y. Jiang, Conversion-alloying anode materials for sodium ion batteries, Small 17 (2021) 2101137.
[6] Y. Xiao, N.M. Abbasi, Y.-F. Zhu, S. Li, S.-J. Tan, W. Ling, L. Peng, T. Yang, L. Wang, X.-D. Guo, Y.-X. Yin, H. Zhang, Y.-G. Guo, Layered oxide cathodes promoted by structure modulation technology for sodium-ion batteries, Adv. Funct. Mater. 30 (2020) 2001334.
[7] J.H. Stansby, N. Sharma, D. Goonetilleke, Probing the charged state of layered positive electrodes in sodium-ion batteries: reaction pathways, stability and opportunities, J. Mater. Chem. A 8 (2020) 24833–24867.
[8] P. Du, L. Cao, B. Zhang, C. Wang, Z. Xiao, J. Zhang, D. Wang, X. Ou, Recent progress on heterostructure materials for next-generation sodium/potassium ion batteries, Renew. Sustain. Energy Rev. 151 (2021) 111640.
[9] Y. Ma, Y. Ma, D. Bresser, Y. Ji, D. Geiger, U. Kaiser, C. Streb, A. Varzi, S. Passerini, Cobalt disulfide nanoparticles embedded in porous carbonaceous micro-polyhedrons interlinked by carbon nanotubes for superior lithium and sodium storage, ACS Nano 12 (2018) 7220–7231.

[10] Q. Pan, M. Zhang, L. Zhang, Y. Li, Y. Li, C. Tan, F. Zheng, Y. Huang, H. Wang, Q. Li, $FeSe_2$@C microrods as a superior long-life and high-rate anode for sodium ion batteries, ACS Nano 14 (2020) 17683–17692.

[11] Y. Zheng, T. Zhou, C. Zhang, J. Mao, H. Liu, Z. Guo, Boosted charge transfer in SnS/SnO_2 heterostructures: toward high rate capability for sodium-ion batteries, Angew. Chem. Int. Ed. 55 (2016) 3408–3413.

[12] T. Ruan, B. Wang, Y. Yang, X. Zhang, R. Song, Y. Ning, Z. Wang, H. Yu, Y. Zhou, D. Wang, H. Liu, S. Dou, Interfacial and electronic modulation via localized sulfurization for boosting lithium storage kinetics, Adv. Mater. 32 (2020) 2000151.

[13] C. Ma, Y. Hou, K. Jiang, L. Zhao, T. Olsen, Y. Fan, J. Jiang, Z. Xu, Z. Ma, D. Legut, H. Xiong, X.-Z. Yuan, In situ cross-linking construction of 3D mesoporous bimetallic phosphide-in-carbon superstructure with atomic interface toward enhanced sodium ion storage performance, Chem. Eng. J. 413 (2021) 127449.

[14] R. He, J. Hua, A. Zhang, C. Wang, J. Peng, W. Chen, J. Zeng, Molybdenum disulfide–black phosphorus hybrid nanosheets as a superior catalyst for electrochemical hydrogen evolution, Nano Lett. 17 (2017) 4311–4316.

[15] Y. Jiang, D. Song, J. Wu, Z. Wang, S. Huang, Y. Xu, Z. Chen, B. Zhao, J. Zhang, Sandwich-like SnS_2 with expanded interlayer distance as high-rate lithium/sodium-ion battery anode materials, ACS Nano 13 (2019) 9100–9111.

[16] Q. Peng, K. Hu, B. Sa, J. Zhou, B. Wu, X. Hou, Z. Sun, Unexpected elastic isotropy in a black phosphorene/TiC_2 van Der Waals heterostructure with flexible Li-ion battery anode applications, Nano Res. 10 (2017) 3136–3150.

[17] Z. Chen, D. Yin, M. Zhang, Sandwich-like MoS_2@SnO_2@C with high capacity and stability for sodium/potassium ion batteries, Small 14 (2018) 1703818.

[18] L. Cui, C. Tan, Y. Li, Q. Pan, L. Zhang, M. Zhang, Z. Chen, F. Zheng, H. Wang, Q. Li, Hierarchical Fe_2O_3@MoS_2/C nanorods as anode materials for sodium ion batteries with high cycle stability, ACS Appl. Energy Mater. 4 (2021) 3757–3765.

[19] J. Zong, F. Wang, C. Nie, M. Zhao, S. Yang, Cobalt and oxygen double doping induced C@MoS_2–CoS_2–O@C nanocomposites with an improved electronic structure and increased active sites as a high-performance anode for sodium-based dual-ion batteries, J. Mater. Chem. A 10 (2022) 10651–10661.

[20] C. Ma, Z. Xu, J. Jiang, Z. Ma, T. Olsen, H. Xiong, S. Wang, X.-Z. Yuan, Tailored nanoscale interface in a hierarchical carbon nanotube supported MoS_2@MoO_2-C electrode toward high performance sodium ion storage, J. Mater. Chem. A 8 (2020) 11011–11018.

[21] Y. Li, H. Wang, L. Xie, Y. Liang, G. Hong, H. Dai, MoS_2 nanoparticles grown on graphene: an advanced catalyst for the hydrogen evolution reaction, J. Am. Chem. Soc. 133 (2011) 7296–7299.

[22] Y. Li, R. Zhang, W. Zhou, X. Wu, H. Zhang, J. Zhang, Hierarchical MoS_2 hollow architectures with abundant Mo vacancies for efficient sodium storage, ACS Nano 13 (2019) 5533–5540.

[23] B. Chen, H. Lu, J. Zhou, C. Ye, C. Shi, N. Zhao, S.-Z. Qiao, Porous MoS_2/carbon spheres anchored on 3D interconnected multiwall carbon nanotube networks for ultrafast Na storage, Adv. Energy Mater. 8 (2018) 1702909.

[24] M.-C. Liu, H. Zhang, Y.-X. Hu, C. Lu, J. Li, Y.-G. Xu, L.-B. Kong, Special layer-structured WS_2 nanoflakes as high performance sodium ion storage materials, Sustain. Energy Fuels 3 (2019) 1239–1247.

[25] S. He, F. Guo, Q. Yang, H. Mi, J. Li, N. Yang, J. Qiu, Design and fabrication of hierarchical NiCoP–MOF heterostructure with enhanced pseudocapacitive properties, Small 17 (2021) 2100353.

[26] Z. Ali, M. Asif, T. Zhang, X. Huang, Y. Hou, General approach to produce nanostructured binary transition metal selenides as high-performance sodium ion battery anodes, Small Weinh. Bergstr. Ger. 15 (2019) e1901995.

[27] B. Qin, H. Zhang, T. Diemant, X. Dou, D. Geiger, R.J. Behm, U. Kaiser, A. Varzi, S. Passerini, Exploring SnS nanoparticles interpenetrated with high concentration nitrogen-doped-carbon as anodes for sodium ion batteries, Electrochim. Acta 296 (2019) 806.

[28] L. Shen, S. Shi, S. Roy, X. Yin, W. Liu, Y. Zhao, Recent advances and optimization strategies on the electrolytes for hard carbon and P-based sodium-ion batteries, Adv. Funct. Mater. 31 (2021) 2006066.

[29] J.-Y. Hwang, H.-L. Du, B.-N. Yun, M.-G. Jeong, J.-S. Kim, H. Kim, H.-G. Jung, Y.-K. Sun, Carbon-free TiO_2 microspheres as anode materials for sodium ion batteries, ACS Energy Lett. 4 (2019) 494–501.

[30] H. Jin, T. Zhang, C. Chuang, Y.-R. Lu, T.-S. Chan, Z. Du, H. Ji, L. Wan, Synergy of black phosphorus–graphite–polyaniline-based ternary composites for stable high reversible capacity Na-ion battery anodes, ACS Appl. Mater. Interfaces 11 (2019) 16656–16661.

[31] G.-L. Xu, Z. Chen, G.-M. Zhong, Y. Liu, Y. Yang, T. Ma, Y. Ren, X. Zuo, X.-H. Wu, X. Zhang, K. Amine, Nanostructured black phosphorus/ketjenblack–multiwalled carbon nanotubes composite as high performance anode material for sodium-ion batteries, Nano Lett. 16 (2016) 3955–3965.

[32] H. Jin, H. Wang, Z. Qi, D.-S. Bin, T. Zhang, Y. Wan, J. Chen, C. Chuang, Y.-R. Lu, T.-S. Chan, H. Ju, A.-M. Cao, W. Yan, X. Wu, H. Ji, L.-J. Wan, A black phosphorus–graphite composite anode for Li-/Na-/K-ion batteries, Angew. Chem. Int. Ed. 59 (2020) 2318–2322.

[33] H. Jiang, D. Ren, H. Wang, Y. Hu, S. Guo, H. Yuan, P. Hu, L. Zhang, C. Li, 2D monolayer MoS_2–carbon interoverlapped superstructure: engineering ideal atomic interface for lithium ion storage, Adv. Mater. 27 (2015) 3687–3695.

[34] C. Ma, X. Li, C. Deng, Y.-Y. Hu, S. Lee, X.-Z. Liao, Y.-S. He, Z.-F. Ma, H. Xiong, Coaxial carbon nanotube supported TiO_2/MoO_2@Carbon core–shell anode for ultrafast and high-capacity sodium ion storage, ACS Nano 13 (2019) 671–680.

[35] J. Jamnik, J. Maier, Nanocrystallinity effects in lithium battery materials, Phys. Chem. Chem. Phys. 5 (2003) 5215–5220.

[36] C. Wang, G. Li, H. Qin, Z. Xiao, D. Wang, B. Zhang, X. Ou, Y. Wu, Strain engineering of layered heterogeneous structure via self-evolution confinement for ultrahigh-rate cyclic sodium storage, Adv. Energy Mater. 12 (2022) 2200403.

[37] H. Zhang, I. Hasa, S. Passerini, Sodium-ion batteries: beyond insertion for Na-ion batteries: nanostructured alloying and conversion anode materials (Adv. Energy Mater. 17/2018), Adv. Energy Mater. 8 (2018) 1870082.

[38] L. Ye, M. Liao, H. Sun, Y. Yang, C. Tang, Y. Zhao, L. Wang, Y. Xu, L. Zhang, B. Wang, F. Xu, X. Sun, Y. Zhang, H. Dai, P.G. Bruce, H. Peng, Stabilizing lithium into cross-stacked nanotube sheets with an ultra-high specific capacity for lithium oxygen batteries, Angew Chem. Int. Ed. 58 (2019) 2437–2442.

[39] R. Zhao, Z. Qian, Z. Liu, D. Zhao, X. Hui, G. Jiang, C. Wang, L. Yin, Molecular-level heterostructures assembled from layered black phosphorene and Ti_3C_2 MXene as superior anodes for high-performance sodium ion batteries, Nano Energy 65 (2019) 104037.

[40] P. Liu, J. Han, K. Zhu, Z. Dong, L. Jiao, Heterostructure $SnSe_2$/ZnSe@PDA nanobox for stable and highly efficient sodium-ion storage, Adv. Energy Mater. 10 (2020) 2000741.

[41] P. Barpanda, L. Lander, S. Nishimura, A. Yamada, Polyanionic insertion materials for sodium-ion batteries, Adv. Energy Mater. 8 (2018) 1703055.

[42] B. Zhang, K. Ma, X. Lv, K. Shi, Y. Wang, Z. Nian, Y. Li, L. Wang, L. Dai, Z. He, Recent advances of NASICON-$Na_3V_2(PO_4)_3$ as cathode for sodium-ion batteries: synthesis, modifications, and perspectives, J. Alloys Compd. 867 (2021) 159060.

[43] Q. Zhou, L. Wang, W. Li, K. Zhao, M. Liu, Q. Wu, Y. Yang, G. He, I.P. Parkin, P.R. Shearing, D.J.L. Brett, J. Zhang, X. Sun, Sodium superionic conductors (NASICONs) as cathode materials for sodium-ion batteries, Electrochem. Energy Rev. 4 (2021) 793–823.

[44] J. Peng, W. Zhang, Q. Liu, J. Wang, S. Chou, H. Liu, S. Dou, Prussian blue analogues for sodium-ion batteries: past, present, and future, Adv. Mater. 34 (2022) 2108384.

[45] Q. Liu, Z. Hu, M. Chen, C. Zou, H. Jin, S. Wang, S.-L. Chou, Y. Liu, S.-X. Dou, The cathode choice for commercialization of sodium-ion batteries: layered transition metal oxides versus prussian blue analogs, Adv. Funct. Mater. 30 (2020) 1909530.

[46] X. Chang, Q. Zhu, N. Sun, Y. Guan, R. Wang, J. Zhao, M. Feng, B. Xu, Graphene-bound $Na_3V_2(PO_4)_3$ film electrode with excellent cycle and rate performance for Na-ion batteries, Electrochim. Acta 269 (2018) 282–290.

[47] X. Li, S. Jiang, S. Li, J. Yao, Y. Zhao, T. Bashir, S. Zhou, S. Yang, W. Li, W. Zhu, T. Liu, J. Zhao, L. Gao, Overcoming the rate-determining kinetics of the $Na_3V_2O_2(PO_4)_2F$ cathode for ultrafast sodium storage by heterostructured dual-carbon decoration, J. Mater. Chem. A 9 (2021) 11827–11838.

[48] Y. Liu, D. He, Y. Cheng, L. Li, Z. Lu, R. Liang, Y. Fan, Y. Qiao, S. Chou, A heterostructure coupling of bioinspired, adhesive polydopamine, and porous prussian blue nanocubics as cathode for high-performance sodium-ion battery, Small 16 (2020) 1906946.

[49] C. Deng, P. Skinner, Y. Liu, M. Sun, W. Tong, C. Ma, M.L. Lau, R. Hunt, P. Barnes, J. Xu, H. Xiong, Li-substituted layered spinel cathode material for sodium ion batteries, Chem. Mater. 30 (2018) 8145–8154.

[50] Y.-F. Zhu, Y. Xiao, S.-X. Dou, Y.-M. Kang, S.-L. Chou, Spinel/post-spinel engineering on layered oxide cathodes for sodium-ion batteries, eScience 1 (2021) 13–27.

[51] E. Gabriel, D. Hou, E. Lee, H. Xiong, Multiphase layered transition metal oxide positive electrodes for sodium ion batteries, Energy Sci. Eng. 10 (2022) 1672–1705.

[52] C. Delmas, C. Fouassier, P. Hagenmuller, Structural classification and properties of the layered oxides, Physica B Condens. Matter 99 (1980) 81–85.

[53] G.L. Xu, R. Amine, Y.F. Xu, J.Z. Liu, J. Gim, T.Y. Ma, Y. Ren, C.J. Sun, Y.Z. Liu, X.Y. Zhang, S.M. Heald, A. Solhy, I. Saadoune, W.L. Mattis, S.G. Sun, Z.H. Chen, K. Amine, Insights into the structural effects of layered cathode materials for high voltage sodium-ion batteries, Energy Environ. Sci. 10 (2017) 1677–1693.

[54] C. Zhao, Q. Wang, Z. Yao, J. Wang, B. Sánchez-Lengeling, F. Ding, X. Qi, Y. Lu, X. Bai, B. Li, H. Li, A. Aspuru-Guzik, X. Huang, C. Delmas, M. Wagemaker, L. Chen, Y.-S. Hu, Rational design of layered oxide materials for sodium-ion batteries, Science 370 (2020) 708–711.

[55] J. Chen, L. Li, L. Wu, Q. Yao, H. Yang, Z. Liu, L. Xia, Z. Chen, J. Duan, S. Zhong, Enhanced cycle stability of $Na_{0.9}Ni_{0.45}Mn_{0.55}O_2$ through tailoring O3/P2 hybrid structures for sodium-ion batteries, J. Power Sources 406 (2018) 110–117.

[56] S. Guo, Q. Li, P. Liu, M. Chen, H. Zhou, Environmentally stable interface of layered oxide cathodes for sodium-ion batteries, Nat. Commun. 8 (2017) 135.

[57] B. Xiao, X. Liu, M. Song, X. Yang, F. Omenya, S. Feng, V. Sprenkle, K. Amine, G. Xu, X. Li, D. Reed, A general strategy for batch development of high-performance and cost-effective sodium layered cathodes, Nano Energy 89 (2021) 106371.

[58] Z. Liu, K. Jiang, S. Chu, J. Wu, H. Xu, X. Zhang, P. Wang, S. Guo, H. Zhou, Integrating P2 into O′3 toward a robust Mn-based layered cathode for sodium-ion Batteries, J. Mater. Chem. A 8 (2020) 23820–23826.

[59] B. Hu, F. Geng, C. Zhao, B. Doumert, J. Trébosc, O. Lafon, C. Li, M. Shen, B. Hu, Deciphering the origin of high electrochemical performance in a novel Ti-substituted P2/O3 biphasic cathode for sodium-ion batteries, ACS Appl. Mater. Interfaces 12 (2020) 41485–41494.

[60] S.-Y. Zhang, Y.-J. Guo, Y.-N. Zhou, X.-D. Zhang, Y.-B. Niu, E.-H. Wang, L.-B. Huang, P.-F. An, J. Zhang, X.-A. Yang, Y.-X. Yin, S. Xu, Y.-G. Guo, P3/O3 integrated layered oxide as high-power and long-life cathode toward Na-ion batteries, Small 17 (2021) 2007236.

[61] E. Lee, J. Lu, Y. Ren, X. Luo, X. Zhang, J. Wen, D. Miller, A. DeWahl, S. Hackney, B. Key, D. Kim, M.D. Slater, C.S. Johnson, Layered P2/O3 intergrowth cathode: toward high power Na-ion batteries, Adv. Energy Mater. 4 (2014) 1400458.

[62] N. Jiang, Q. Liu, J. Wang, W. Yang, W. Ma, L. Zhang, Z. Peng, Z. Zhang, Tailoring P2/P3 biphases of layered Na_xMnO_2 by Co substitution for high-performance sodium-ion battery, Small 17 (2021) 2007103.

[63] Z. Yan, L. Tang, Y. Huang, W. Hua, Y. Wang, R. Liu, Q. Gu, S. Indris, S.-L. Chou, Y. Huang, M. Wu, S.-X. Dou, A hydrostable cathode material based on the layered P2@P3 composite that shows redox behavior for copper in high-

rate and long-cycling sodium-ion batteries, Angew. Chem. Int. Ed. 58 (2019) 1412–1416.
[64] Y.S. Wang, R.J. Xiao, Y.S. Hu, M. Avdeev, L.Q. Chen, P2-Na-0.6[Cr0.6Ti0.4]O-2 Cation-disordered electrode for high-rate symmetric rechargeable sodium-ion batteries, Nat. Commun. 6 (2015) 6954.
[65] L.G. Chagas, D. Buchholz, C. Vaalma, L. Wu, S. Passerini, P-type $Na_xNi_{0.22}Co_{0.11}Mn_{0.66}O_2$ Materials: linking synthesis with structure and electrochemical performance, J. Mater. Chem. A 2 (2014) 20263–20270.
[66] Q. Huang, M. Wang, L. Zhang, S. Qi, Y. Feng, P. He, X. Ji, P. Wang, L. Zhou, S. Chen, W. Wei, Shear-resistant interface of layered oxide cathodes for sodium ion batteries, Energy Stor. Mater. 45 (2022) 389–398.
[67] M. Treacy, J. Newsam, M. Deem, A general recursion method for calculating diffracted intensities from crystals containing planar faults, Proc. R. Soc. Lond. Ser. Math. Phys. Sci. 433 (1991) 499–520.
[68] M. Casas-Cabanas, M. Reynaud, J. Rikarte, P. Horbach, J. Rodriguez-Carvajal, Faults: A program for refinement of structures with extended defects, J. Appl. Crystallogr. 49 (2016) 2259–2269.
[69] K. Kubota, N. Fujitani, Y. Yoda, K. Kuroki, Y. Tokita, S. Komaba, Impact of Mg and Ti doping in O3 type $NaNi_{1/2}Mn_{1/2}O_2$ on reversibility and phase transition during electrochemical Na intercalation, J. Mater. Chem. A 9 (2021) 12830–12844.
[70] Z. Lu, J. Dahn, Effects of stacking fault defects on the X-ray diffraction patterns of T2, O2, and O6 structure $Li_{2/3}[Co_xNi_{1/3-x}Mn_{2/3}]O_2$, Chem. Mater. 13 (2001) 2078–2083.
[71] G.K. Williamson, W.H. Hall, X-ray line broadening from filed aluminium and wolfram, Acta Metall. 1 (1953) 22–31.
[72] D. Hou, D. Xia, E. Gabriel, J.A. Russell, K. Graff, Y. Ren, C.-J. Sun, F. Lin, Y. Liu, H. Xiong, Spatial and temporal analysis of sodium-ion batteries, ACS Energy Lett. 6 (2021) 4023–4054.